Proceedings of the Combustion Institute

Micron-sized iron particles as energy carrier: Cycling experiments in a fixed-bed reactor

--Manuscript Draft--

Manuscript Number:	
Article Type:	Vol. 40: Manuscript
Section/Category:	413: Low-Carbon Technologies
Keywords:	Energy storage; Iron particles; Oxidation behavior; Cyclization; Fixed-bed reactor
Manuscript Classifications:	413: Low-Carbon Technologies
Corresponding Author:	Olaf Deutschmann, Dr. Karlsruhe Institute of Technology Karlsruhe, GERMANY
First Author:	Carola Kuhn
Order of Authors:	Carola Kuhn
	Marco Kirn
	Steffen Tischer, Dr.
	Olaf Deutschmann, Dr.
Abstract:	Iron is a promising energy carrier with the potential to store substantial amounts of energy over extended time periods with minimal losses. For instance, the energy from green hydrogen sources can be used to reduce iron oxides, be stored or transported, and thus be regained by exothermic oxidation of the iron. This work explores the influence of oxygen partial pressure and temperature on the oxidation process in a fixed-bed reactor. Furthermore, the analysis extends to the reduction of oxidized iron particles at varying temperatures. The experimental findings highlight that both oxidation and reduction progress through the fixed-bed reactor as distinct reaction fronts. In the oxidation process, the speed of the reaction front increases with rising oxygen content and temperature, resulting in a higher reaction rate and a correspondingly increased heat release. Conversely, the reaction rate for reduction experiences a notable decrease for 600 °C and 700 °C. The reprocessability of the iron powder was validated for up to 16 cycles under the optimal reaction conditions established. Furthermore, it was demonstrated that the performance improves with an increasing number of cycles. This improvement is attributed to the formation of pores due to density changes and the subsequent creation of a larger surface area, mitigating the negative effects of sintering and agglomeration.
Additional Information:	

Question	Response
Are you submitting for consideration as an Oral Presentation or Poster Paper Presentation?	Oral Presentation
Please highlight the novelty and contribution of this paper in 3-5 brief statements:	In-depth analysis of micron-sized iron powder in a fixed-bed reactor, considering oxidation, reduction and cyclization Oxidation and reduction progress through the fixed-bed reactor as reaction fronts Formation of pores counteracts the decreased reaction rate due to sintering Improved performance with increasing number of cycles

Micron-sized iron particles as energy carrier: Cycling experiments in a fixed-bed reactor

Carola Kuhn[a], Marco Kirn[a], Steffen Tischer[b], Olaf Deutschmann[a,b,*]

[a] *Institute for Chemical Technology and Polymer Chemistry, Karlsruhe Institute of Technology, Engesserstr. 20, 76131 Karlsruhe, Germany*
[b] *Institute of Catalysis Research, Karlsruhe Institute of Technology, Hermann-von-Helmholtz-Platz 1, 76344 Eggenstein-Leopoldshafen, Germany*

Abstract

Iron is a promising energy carrier with the potential to store substantial amounts of energy over extended time periods with minimal losses. For instance, the energy from green hydrogen sources can be used to reduce iron oxides, be stored or transported, and thus be regained by exothermic oxidation of the iron. This work explores the influence of oxygen partial pressure and temperature on the oxidation process in a fixed-bed reactor. Furthermore, the analysis extends to the reduction of oxidized iron particles at varying temperatures. The experimental findings highlight that both oxidation and reduction progress through the fixed-bed reactor as distinct reaction fronts. In the oxidation process, the speed of the reaction front increases with rising oxygen content and temperature, resulting in a higher reaction rate and a correspondingly increased heat release. Conversely, the reaction rate for reduction experiences a notable decrease for 600 °C and 700 °C. The reprocessability of the iron powder was validated for up to 16 cycles under the optimal reaction conditions established. Furthermore, it was demonstrated that the performance improves with an increasing number of cycles. This improvement is attributed to the formation of pores due to density changes and the subsequent creation of a larger surface area, mitigating the negative effects of sintering and agglomeration.

Keywords: Energy storage; Iron particles; Oxidation behavior; Cyclization; Fixed-bed reactor

Information for Colloquium Chairs and Cochairs, Editors, and Reviewers

1) Novelty and Significance Statement

This study's uniqueness lies in the in-depth investigation of iron powder as an energy carrier within a fixed-bed reactor. The obtained results significantly contribute to an enhanced comprehension of the processes occurring during oxidation and reduction. Moreover, this work demonstrates the feasibility and efficiency of iron powder cyclization on a larger scale.

2) Author Contributions

- C.K.: Conceptualization , analyzed data, writing - original draft
- M.K.: Performed research, analyzed data
- S.T.: Writing - review & editing
- O.D.: Designed research, supervision, writing - review & editing

3) Authors' Preference and Justification for Mode of Presentation at the Symposium

The authors prefer **OPP** presentation at the Symposium, for the following reasons:

- Consideration of the entire process, i.e. energy storage and release, for the utilization of iron as energy carrier.
- In its concluding evaluation of the cyclization, the study builds upon the previously obtained results for oxidation and reduction.
- The results hold significant relevance for the expanding community researching metal fuels, particularly iron.

1. Introduction

The group of reactive metals, including aluminum, silicon, and iron, has received much attention in recent years as carbon-free, recyclable fuels [1–3]. They can store vast amounts of energy with minimal losses for extended periods, thus making them ideal for seasonal energy storage [4]. The corresponding charging and discharging process can be spatially and temporally separated. Energy storage in iron occurs through thermochemical reduction of iron oxides using green hydrogen produced by electrolysis [5]. This is feasible in regions with low-cost renewable energy, notably North Africa or Australia [6]. Energy release is accomplished in regions with high energy demand. Iron is combusted with air, and the resulting heat can be harnessed directly or used to generate electricity [7]. The iron oxides produced during combustion are solid at standard conditions, easily collected, and recyclable. This combination of processes satisfies the demand for a carbon-free energy carrier and supports the principles of the circular economy [8]. Iron powder is of particular interest among reactive metals due to its high volumetric energy density, non-toxicity, ease of transportation, low hazard potential and affordability [3]. Initial studies are exploring the potential of iron particles in energy storage systems. Numerous studies are dedicated to a comprehensive understanding of the processes during oxidation, examining the oxidation of iron particles under mild conditions, on small scales, and within a narrow parameter range [9–11]. The crucial aspect of the oxidation process is marked by an initial rapid phase, followed by a subsequent decrease in the reaction rate. This behavior is ascribed to the development of a dense iron oxide layer, causing a shift in the oxidation mode from the kinetic regime to the diffusion-limited regime [12, 13]. Several studies in literature explore the reduction behavior of iron oxides with hydrogen. However, there is significant variation in the findings of these studies, highlighting the crucial role played by particle properties in the reduction process [14]. Therefore, it is necessary to thoroughly investigate the reduction behavior of oxidized iron particles, which are used in the metal fuel cycle. Nevertheless, research on this topic remains scarce in literature. First studies revealed that the reduction process of combusted iron particles exhibits a pronounced temperature dependence [15, 16]. Additionally, it was demonstrated that the reduction induces changes in particle morphology. Previous studies indicate that alterations in particle morphology, can significantly impact both oxidation and reduction behavior [13, 17]. The objective of this work is to conduct a comprehensive investigation of the oxidation and reduction processes within the iron/iron oxide system using a fixed-bed reactor. The results will be employed to determine the ideal conditions for cyclization. Furthermore, the effects of repeated oxidation and reduction on particle properties will be explored through long-term experiments.

2. Experimental

2.1. Fresh iron powder

The analyzed iron powder has an average particle diameter of $23\,\mu\mathrm{m}$. Figure 1 presents the particle size distribution of the powder. Recent research indicates that oxidation and reduction of iron particles results in sintering and agglomeration of the particles [9, 18]. To prevent sintering, the iron powder was mixed with ball-milled quartz sand, in a 1:8 ratio. To investigate the oxidation of iron particles, a $20\,\mathrm{mm}$ bed fixed with quartz wool was obtained by diluting $200\,\mathrm{mg}$ of iron powder with $1600\,\mathrm{mg}$ of quartz sand and placing this mixture in a quartz glass tubular reactor ($8\,\mathrm{mm}$ i.d.). For the reduction and cyclization experiments, $400\,\mathrm{mg}$ of iron powder diluted with quartz sand (1:8) were loaded into a reactor with an inner diameter of $26.4\,\mathrm{mm}$, resulting in a bed length of $2\,\mathrm{mm}$.

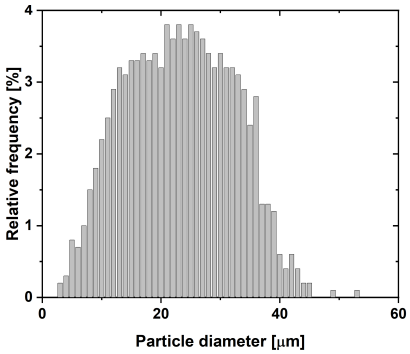

Fig. 1: Particle size distribution of the investigated powder sample. It is taken from [9] as the same powder batch is used.

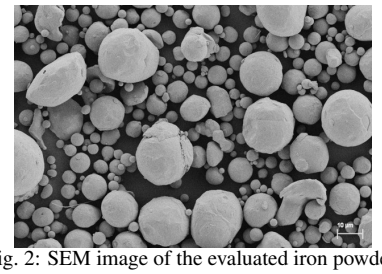

Fig. 2: SEM image of the evaluated iron powder.

2.2. Analysis of the iron powder performance

The loaded reactor was placed in a furnace (HTM Reetz GmbH) for uniform heating. For all experiments, the temperature was monitored by two thermocouples placed upstream and downstream of the fixed-bed. Reactor heating and cooling was controlled by Eurotherm controllers using the thermocouple located upstream of the fixed-bed. Reaction

gases were dosed by Bronkhorst Mass Flow Controllers. The reduction product water was monitored by a FTIR spectrometer (MKS Instruments). Oxidation experiments were performed at a flow rate of $150\,\mathrm{mL\,min^{-1}}$, unless otherwise noted. The oxygen content was varied from $5\,\%$ to $30\,\%$ balanced with nitrogen. To minimize errors in the analysis of product gases via FTIR, a higher volume flow is utilized. Therefore, all reduction experiments were conducted with a total volume flow of $500\,\mathrm{mL\,min^{-1}}$ and $5\,\%$ H_2 in N_2. In the cyclization experiments each oxidation and reduction was followed by purging with $500\,\mathrm{mL\,min^{-1}}$ of nitrogen for $15\,\mathrm{min}$. Additionally, the cycling behavior was analyzed based on thermogravimetric experiments (Netzsch STA409). Around $10\,\mathrm{mg}$ iron powder were used for each experiment. Oxidation was performed at $650\,^{\circ}\mathrm{C}$ with synthetic air and reduction at $500\,^{\circ}\mathrm{C}$ with $5\,\%$ H_2 balanced with N_2 both with a volume flux of $100\,\mathrm{mL\,min^{-1}}$. Transition between oxidation and reduction was performed at $15\,\mathrm{K\,min^{-1}}$ with $200\,\mathrm{mL\,min^{-1}}$ N_2.

3. Results and discussion

3.1. Oxidation

Due to the exothermic nature of iron oxidation, the rise in temperature enables the monitoring of the process. The temperature was measured with a thermocouple located $5\,\mathrm{mm}$ downstream of the fixed-bed. In order to improve the comparability of the individual measurements, the actual measured temperatures were normalized by subtracting the average temperature prior to the start of the oxidation. The effect of temperature on oxidation is shown in Figure 3. This was investigated at a total flow rate of $50\,\mathrm{mL\,min^{-1}}$ and an O_2 concentration of $10\,\%$. All measurements, except the one taken at $500\,^{\circ}\mathrm{C}$, indicate a decrease in temperature following the initiation of the reaction. The cause of this phenomenon is attributable to the structure of the control circuit. The reference thermocouple is positioned in front of the fixed-bed. When oxidation begins, the temperature upstream of the fixed-bed initially increases. This causes the control circuit to counteract the registered temperature increase by slightly reducing the furnace power. The subsequent temperature rise is dependent on the initial temperature. A higher initial temperature results in a higher maximum temperature of the exhaust gas. At $500\,^{\circ}\mathrm{C}$, oxidation causes a temperature increase of $1.5\,\mathrm{K}$, while at $750\,^{\circ}\mathrm{C}$ the increase is $9.5\,\mathrm{K}$. The increase in temperature of the exhaust gas is followed by a prompt and significant decrease to its original temperature, indicating a distinct drop of the reaction rate. This may be caused by a transition from the kinetically controlled reaction regime to the diffusion controlled reaction regime. This phenomenon is likely due to the formation of an iron oxide layer in the initial oxidation stage, resulting in the diffusion of iron cations through the Fe_2O_3/Fe_3O_4 layer being the rate-limiting step. The delay in reaching the highest exhaust air temperature, which correlates with the oxidation temperature, may be attributed to the formation of a reaction front. The initial oxidation occurring in the front section of the fixed-bed reduces the amount of oxygen reaching the rear section of the bed. The higher the temperature, the more of the available oxygen is consumed. However, as the oxygen flow remains constant, the oxidation front takes longer to reach the end of the fixed-bed at higher temperatures. Near the end of the bed, the heat dissipation is high enough to heat the exhaust stream sufficiently to measure a temperature difference.

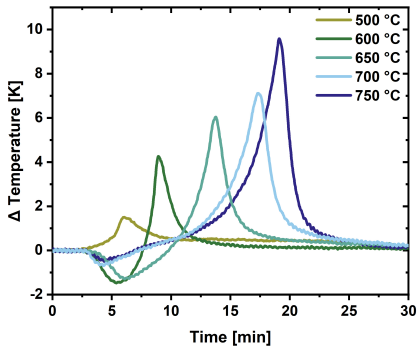

Fig. 3: Temperature increase during iron powder oxidation at temperatures ranging from $500\,^{\circ}\mathrm{C}$ to $750\,^{\circ}\mathrm{C}$ with a total volumetric flow of $50\,\mathrm{mL\,min^{-1}}$ and 10 vol.–% O_2.

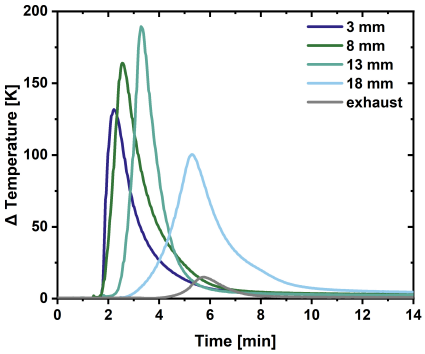

Fig. 4: Temperature profile during iron powder oxidation at $650\,^{\circ}\mathrm{C}$ with a total volumetric flow of $150\,\mathrm{mL\,min^{-1}}$ and 21 vol.–% O_2.

In order to better understand the processes occurring in the fixed-bed during iron powder oxidation, a temperature profile of the fixed-bed was obtained by repeating the experiment under identical conditions ($650\,^{\circ}\mathrm{C}$, $150\,\mathrm{mL\,min^{-1}}$, $21\,\%$ O_2). A type K thermocouple with a width of $0.25\,\mathrm{mm}$ was inserted into a capillary placed in the center of the fixed-bed. The temperature was measured at four positions with a distance of $5\,\mathrm{mm}$. The results are shown in Fig. 4. The temperature profile substantiates the hypothesis regarding the formation of a reaction front. Evidently, the temperature within the bed exhibits a tem-

poral offset along the longitudinal axis, indicating the progression of the reaction. Moreover, the observed temperature peak rises proportionally with the bed length. This phenomenon can be ascribed to the effective transfer of heat generated by the ongoing reaction to successive particles. Consequently, the oxidation initiates at a higher initial temperature, resulting in enhanced conversion rates and, consequently, augmented heat release. Notably, a temperature difference of 60 K is observed between position 1 and position 3. Furthermore, temperature measurements within the fixed-bed reveal a substantial disparity between the temperature increase recorded in the exhaust gas and the actual temperature rise. While a maximum temperature increase of merely 15 K is detected in the exhaust gas, the internal fixed-bed experiences a remarkable temperature rise of 190 K. This phenomenon can be ascribed to a significant radial heat loss. In addition to temperature variations, the impact of oxygen partial pressure on the oxidation of iron particles was investigated. Maintaining a total volume flow of $50\,\mathrm{mL\,min^{-1}}$ and an oxidation temperature of 600 °C, the oxygen content was systematically varied from 5 % to 30 % (Fig. 5). The study revealed that the heat released by the reaction increased with higher O_2 concentrations. Concurrently, the time required to reach the maximum temperature decreased as the oxygen concentration increased. The oxidation conducted with 5 vol.–% O_2 does not exhibit a measurable temperature increase. After 120 min of oxidation, a noticeable color differentiation becomes evident within the fixed-bed (Fig. 5). XRD analysis of the lower section of the fixed-bed revealed clear diffractions corresponding to $\alpha-$Fe, Fe_3O_4 and Fe_2O_3. In contrast, the upper half displays diffractions exclusively related to $\alpha-$Fe. This implies that the oxidation front has completely consumed the available oxygen in the feed gas during the initial oxidation. A direct correlation is observed between the oxygen availability and the released heat, with a corresponding increase of the degree of oxidation. Furthermore, an excess of oxygen accelerates the advancement of the oxidation front within the reactor, attributable to the increased oxidation rate induced by the surplus oxygen.

3.2. Reduction

The recycling of iron oxide particles and energy storage occurs through their reduction with hydrogen. The effect of temperature on the reduction process was investigated on oxidized iron particles. The oxidation parameters were carefully selected to ensure complete conversion of iron to iron oxide. In order to achieve this, the iron powder was oxidized for 120 min at a temperature of 650 °C, using a volumetric flow rate of $150\,\mathrm{mL\,min^{-1}}$ with 21 vol.–% O_2. The reduction using a gas mixture of 5 % H_2 in N_2 was performed at temperatures ranging from 400 °C to 900 °C. The progression of the reduction can be observed through the generation of H_2O and

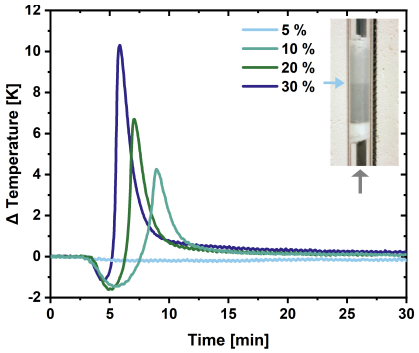

Fig. 5: Development of the exhaust gas temperature as oxygen content varies between 5 % and 30 % at 600 °C with a total volumetric flow of $50\,\mathrm{mL\,min^{-1}}$. The image shows the fixed-bed after 120 min of oxidation with 5 vol.–% O_2.

measured via FTIR. The results are shown in Fig. 6a. At 400 °C, the water concentration in the gas stream rises to 0.2 vol.–% and maintains a consistent level throughout the entire reaction. At 500 °C and 600 °C, the reduction process follows a distinctive two-step behavior. Initially, there is a rapid increase in water concentration, corresponding to an accelerated reduction rate. At 500 °C, the peak water production reaches 1 %, whereas at 600 °C, it rises to 2.6 %. Subsequently, the reduction rate experiences a steep decline, particularly at 600 °C. The water concentration stabilizes for both temperatures during the latter phase. However, at 600 °C, it gradually decreases and approaches zero after approximately 50 min. An additional plateau is observable at elevated temperatures, particularly at 700 °C and 800 °C. Furthermore, the maximum water concentration reaches up to 4.1 % at 800 °C and 900 °C, with a slightly lower value of 3.8 % at a reduction temperature of 700 °C. A comparable pattern in the reduction of iron oxides within fixed-bed reactors was noted by Hertel at al. [19]. In their study, however, the investigation was limited to the reduction process starting from Fe_3O_4. They characterized this behavior as a typical breakthrough phenomenon observed in fixed-bed reactors. The reduction of Fe_2O_3 can be divided into a two- or three-stage mechanism depending on the reduction temperature. At temperatures below 570 °C, Fe_2O_3 is reduced to iron via Fe_3O_4 serving as an intermediate. At temperatures above 570 °C, FeO is formed as an intermediate prior to the formation of Fe. Hertel et al. [19] suggests that the reaction steps within a fixed-bed reactor can be categorized into distinct reaction zones separated by reaction fronts. The measured concentrations of water can then be linked to the breakthrough of these reaction zones, such as $Fe_3O_4 \longrightarrow$ FeO. The concentration between the reaction fronts should correspond to the equilibrium concentration of the gas phase. Applied to the results of this study, it can be deduced that the reduction process at 700 °C comprises three

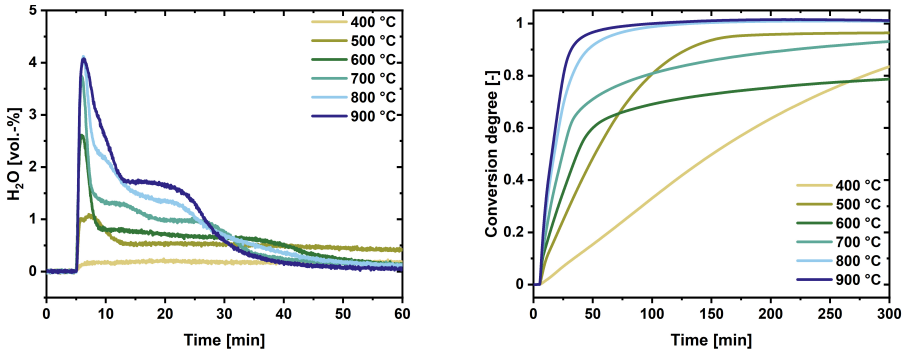

(a) (b)

Fig. 6: a) Water content in the exhaust gas for the isothermal reduction with 5 % H_2 at temperatures from 400 °C to 900 °C and b) the resulting conversion degree.

distinct stages. The initial peak corresponds to the reduction of Fe_2O_3 to Fe_3O_4, the subsequent peak corresponds to the reduction of Fe_3O_4 to FeO, and the final peak represents the complete reduction to Fe. Nevertheless, upon closer examination of the water concentrations, it is evident that they are significantly lower than the equilibrium concentration [20], indicating kinetically or transport limited reduction. This suggests that the reduction occurs stepwise but is influenced by other processes, e.g. solid state diffusion processes. To obtain a more comprehensive understanding of the ongoing reduction process, the conversion degree of Fe_2O_3 over time was calculated for each experiment. The degree of conversion is determined by the ratio of the actual quantity of water generated to the theoretically maximum amount of water that would be produced by a complete reduction. The results are shown in Fig. 6b. Significant temperature-dependent differences are evident when comparing the conversion degree. At 400 °C, the conversion degree increases approximately linearly over time. In the range of 500 °C to 700 °C, there is a noticeable rise in the initial degree of conversion as the temperature increases. For the 600 °C and 700 °C plots, a marked drop in the conversion rate occurs at around 60 % conversion, indicating that, despite a 300 min reduction period, complete reduction was not achieved. The conversion rate at the highest temperatures of 800 °C and 900 °C primarily follows a linear pattern, deviating only shortly before full reduction is attained. The abrupt decrease in the reduction rate at 600 °C and 700 °C results in a comparatively higher conversion rate being achieved at the lower temperatures of 400 °C and 500 °C within the same time frame. Similar observations regarding the reduction of combusted iron particles were reported by Hessels et al. [16]. They noted a shift in the reduction behavior for temperatures higher than 600 °C compared to lower temperatures. At lower temperatures, they observed a gradual but continuous reduction, while at $T > 600\,°C$, the reduction displayed a significantly reduced reaction rate, similar to the findings in this study. They proposed that the reduction slowdown is a consequence of FeO formation and a shift of the reaction mechanism from boundary-controlled to a mechanism limited by nucleation and growth processes.

3.3. Cyclization

The potential for cyclization without substantial efficiency losses is a crucial factor for utilizing iron as energy carrier. Cyclization is studied through short and long-term experiments, using optimal process parameters for high reversibility and efficiency. Oxidation is conducted at 650 °C with a volume flow of 150 mL min^{-1} and 21 % O_2. A temperature of 500 °C is selected for the reduction phase due to its superior reduction rate compared to higher temperatures. Cyclization experiments were conducted with 1, 2, 4, 8, and 16 cycles to ensure reproducibility and enable the analysis of particle morphology in relation to the cycle number. The results are shown in Fig. 7a. The black line represents the quantity of water formed during the reduction in the experiment involving 16 cycles. The symbols correspond to the degree of conversion during the reduction process of all cyclization experiments. A conversion degree of one corresponds to the maximum amount of water theoretically achievable through the complete reduction of the weighed iron powder. The experimental results suggest a high degree of consistency in the conversion rate. The initial peak of the water content consistently rises with each cycle, whereas the reduction time notably decreases only in the first two cycles. Following that, the final conversion degree is achieved slightly earlier in the subsequent cycles. The attained conversion degrees demonstrate a sharp decrease of over 7 % in the second cycle but rapidly recover, approaching the maximum achievable degree of conversion within four cycles. From the 7th cycle onward, complete conversion is consistently achieved without any discernible loss of reactivity. From the obtained results, it cannot be definitively concluded whether the de-

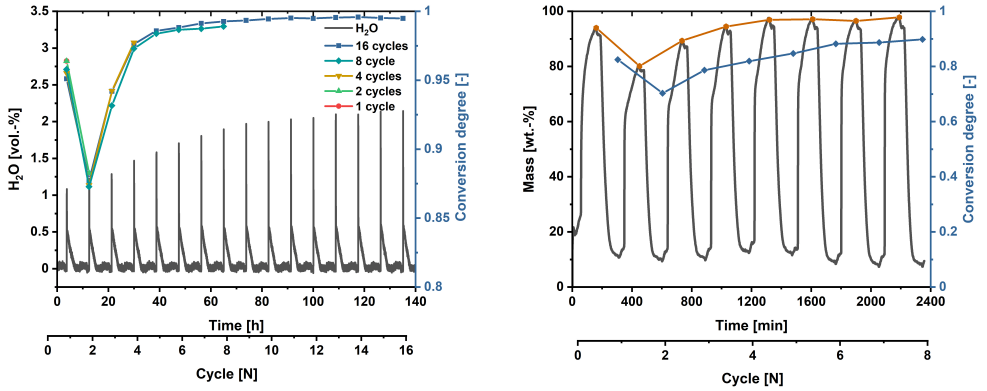

(a) (b)

Fig. 7: a) Water content in the exhaust gas flow during the cyclization of iron powder and the degree of reduction achieved over time. b) Evolution of the weight change during oxidation and reduction in thermogravimetric experiments and the resulting oxidation conversion (orange symbols) and reduction conversion (blue symbols) over time.

cline in the second cycle is attributed to incomplete reduction or if the preceding oxidation process was not fully completed. Based on this, thermogravimetric experiments were conducted under identical conditions, involving oxidation at 650 °C with 21 % O_2, followed by reduction at 500 °C with 5 % H_2. These experiments enable the tracking of both reduction and oxidation processes. The outcomes for 8 cycles are illustrated in Figure 7b. The black line illustrates the variation in mass during the reaction, where 0 % corresponds to pure iron, and 100 % represents a fully oxidized sample, i.e. pure Fe_2O_3. The abrupt change in mass increase/decrease observed between oxidation and reduction can be attributed to the cooling or heating of the furnace. For each oxidation and reduction segment, the conversion degree is calculated relative to the initial iron mass. This is depicted in Fig. 7b, with the oxidation conversion degree represented by the orange symbols and the reduction conversion degree in blue. The reduction times were shortened for the TGA experiments, accounting for the generally lower degree of conversion. However, a decrease in conversion in the second cycle is also observable in the TGA experiments. The conversion degree increases after the second cycle and stabilizes at approximately 0.9 for the reduction from the 6th cycle onwards. To enhance the overall understanding of the process, Fig. 8 displays the superimposed results of each cycle. The results reveal that the second oxidation results in a notably lower oxidation degree, in contrast to the first cycle. Subsequent oxidations achieve a degree of conversion that increases with the number of cycles in the same time frame and approximately the same initial state. The oxidation process undergoes a shift whereby the rapid initial oxidation observed in the first cycle is followed by a nearly linear increase in sample mass from the second cycle onwards. The conversion degree achieved during the initial oxidation rises with increasing cycle number. The reduction curves demonstrate minimal variance across cycles. Only a marginal rise in the reduction rate is perceptible with an increasing number of cycles. Moreover, the reduction for each cycle experiences a significant slowdown at a conversion rate of 0.1 and complete reduction is not attained for any cycle. This illustrates that the decrease of the conversion degree in the second cycle and the subsequent increase are influenced by processes that have a greater impact on oxidation than on reduction. The decrease in conversion in the second cycle might be caused by sintering. Calvo et al. [17] examined the cycling performance of undiluted iron powders. Their results indicated a substantial improvement in conversion during the first four cycles. In contrast to the present study, however, the conversion degree consistently declined in the subsequent cycles and could only be increased by extending the oxidation time. The authors attributed the diminishing reactivity to an increasing sintering effect and the potential for increased agglomeration.

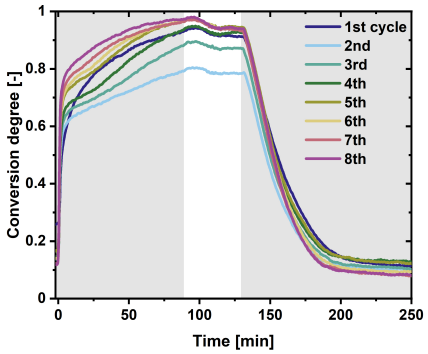

Fig. 8: Cyclization of the iron powder sample in a TGA. The oxidation is conducted in synthetic air at 650 °C and the reduction with 5 % H_2 at 500 °C.

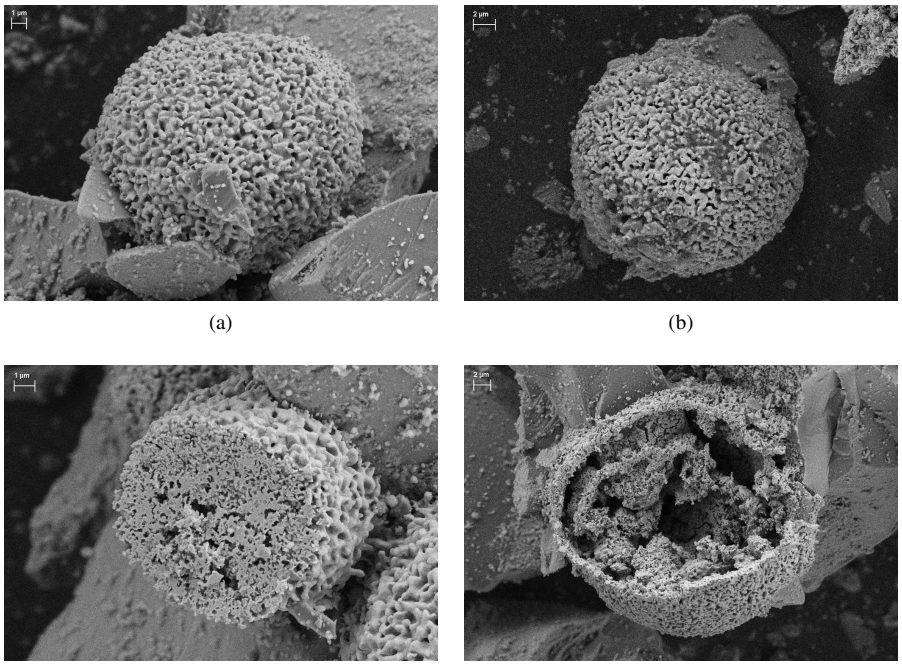

(a) (b)

(c) (d)

Fig. 9: SEM images of iron particles after a) one and b) eight cycles. Cross-sectional image of a reduced particle c) after one cycle and d) after eight cycles.

For a more comprehensive understanding and detailed insight, SEM images of the reduced particles were taken after one and eight cycles. The images are presented in Figure 9. The SEM images reveal that cyclization induces a substantial alteration in the surface structure. The surface of the initial particles appears smooth with no evident pores (Fig. 2). After one cycle, the particles exhibit a rough surface structure, and smaller pores become discernible, suggesting a sponge-like structure. Comparing particles after one and eight cycles shows no significant differences in the surface structure (Fig. 9a and b). Some particles with open structures were identified in the samples. Figure 9c and d depicts the cross-section of a particle after one cycle and the internal structure of a particle after eight cycles. The cross-section of the particle in Fig.9c demonstrates that numerous pores of varying sizes are present inside the particle after the first cycle. Additionally, larger cavities and pores are observed in the particle core compared to the outer area. Superficial pores extend deep into the particle, forming channels that interconnect internal pores. These pores and channels enhance gas accessibility in subsequent cycles, creating a higher surface area for heterogeneous reactions. This effect is more prominent for oxidation than for reduction, given the higher diffusivity of hydrogen compared to oxygen. Figure 9d shows an open particle after eight cycles. Its interior features notably large cavities compared to the particle after one cycle. This indicates that cyclization results in an increased porosity, reducing the particle fraction that is not directly accessible to reactive gases. Consequently, with an increasing number of cycles, a larger portion of iron can be converted before the reaction is impeded by solid-state diffusion. The results indicate that the loss of reactivity induced by sintering can be mitigated by an increase in porosity with rising cycle number. This effect is likely to be more pronounced at lower temperatures, as sintering effects tend to intensify with increasing temperature [18].

4. Conclusion

In this study, an in-depth investigation was conducted to analyze the performance of iron as energy carrier. The influence of various parameters on the oxidation behavior was determined in a fixed-bed reactor. The experimental results revealed that oxidation progresses through the reactor as a reaction front, with the speed of the moving front being dependent on temperature and oxygen partial pressure. Additionally, the reduction behavior of oxidized iron particles was investigated. The appearance of a reaction front progressing through the reactor is also observed for the reduction. The characteristics of the reduction, influenced by the formation of the intermediates Fe_3O_4 and FeO, vary with temperature. The experiments indicated a significant decrease in the reduction rate at temperatures above $600\,^{\circ}\mathrm{C}$, presumably attributed to the formation of FeO. Building upon these experiments, the optimal conditions for the cy-

clization of iron powders were determined. Cyclization experiments involving up to 16 cycles were conducted, revealing that the formation of pores and the resulting larger surface area of the particles can counteract the reduction in the reaction rate due to sintering, thereby increasing the conversion with an increasing number of cycles.

Declaration of competing interest

The authors declare that they have no known competing financial interests or personal relationships that could have appeared to influence the work reported in this paper.

Acknowledgments

This work was performed within the cluster project Clean Circles. Financial support by the Strategy Fund of the KIT Presidium is gratefully acknowledged.

Declaration of generative AI and AI-assisted technologies in the writing process

During the preparation of this work the authors used ChatGPT/Open AI in order to improve readability. After using this tool/service, the authors reviewed and edited the content as needed and take full responsibility for the content of the publication.

References

[1] M. Baumann, L. Barelli, S. Passerini, The Potential Role of Reactive Metals for a Clean Energy Transition, Adv. Energy Mater. 10 (27) (2020). doi:10.1002/aenm.202001002.

[2] J. M. Bergthorson, Recyclable metal fuels for clean and compact zero-carbon power, Prog. Energy Combust. Sci. 68 (2018) 169–196. doi:10.1016/j.pecs.2018.05.001.

[3] P. Debiagi, R. C. Rocha, A. Scholtissek, J. Janicka, C. Hasse, Iron as a sustainable chemical carrier of renewable energy: Analysis of opportunities and challenges for retrofitting coal-fired power plants, Renew. Sust. Energy Rev. 165 (2022) 112579. doi:10.1016/j.rser.2022.112579.

[4] L. Dirven, N. G. Deen, M. Golombok, Dense energy carrier assessment of four combustible metal powders, Sustain. Energy Technol. Assess. 30 (2018) 52–58. doi:10.1016/j.seta.2018.09.003.

[5] C. Kuhn, A. Düll, P. Rohlfs, S. Tischer, M. Börnhorst, O. Deutschmann, Iron as recyclable energy carrier: Feasibility study and kinetic analysis of iron oxide reduction, Appl. Energy Combust. Sci. 12 (2022) 100096. doi:10.1016/j.jaecs.2022.100096.

[6] J. Neumann, R. C. Da Rocha, P. Debiagi, A. Scholtissek, F. Dammel, P. Stephan, C. Hasse, Techno-economic assessment of long-distance supply chains of energy carriers: Comparing hydrogen and iron for carbon-free electricity generation, Appl. Energy Combust. Sci. 14 (2023) 100128. doi:10.1016/j.jaecs.2023.100128.

[7] J. Janicka, P. Debiagi, A. Scholtissek, A. Dreizler, B. Epple, R. Pawellek, A. Maltsev, C. Hasse, The potential of retrofitting existing coal power plants: A case study for operation with green iron, Appl. Energy 339 (2023) 120950. doi:10.1016/j.apenergy.2023.120950.

[8] P. Lott, O. Deutschmann, Heterogeneous chemical reactions—A cornerstone in emission reduction of local pollutants and greenhouse gases, Proc. Combust. Inst. 39 (3) (2023) 3183–3215. doi:10.1016/j.proci.2022.06.001.

[9] J. Spielmann, D. Braig, T. Gustmann, F. Rainauer, A. Streck, A. Kurnosov, O. Leubner, V. Potapkin, C. Hasse, B. J. Etzold, Scholtissekm A., U. Kramm, Exploring the oxidation behaviour of iron particles for large scale energy storage, Phys. Chem. Chem. Phys. submitted (2023).

[10] A. V. Korshunov, Kinetics of the oxidation of an electroexplosion iron nanopowder during heating in air, Russ. J. Phys. Chem. B 6 (3) (2012) 368–375. doi:10.1134/S1990793112050053.

[11] E. N. Lysenko, E. V. Nikolaev, V. A. Vlasov, S. P. Zhuravkov, Investigation of oxidation process of mechanically activated ultrafine iron powders, IOP Conf. Ser.: Mater. Sci. Eng. 110 (2016) 012093. doi:10.1088/1757-899X/110/1/012093.

[12] E. N. Lysenko, A. P. Surzhikov, S. P. Zhuravkov, V. A. Vlasov, A. V. Pustovalov, N. A. Yavorovsky, The oxidation kinetics study of ultrafine iron powders by thermogravimetric analysis, J. Therm. Anal. Calorim. 115 (2) (2014) 1447–1452. doi:10.1007/s10973-013-3456-x.

[13] C. Kuhn, A. Knapp, M. P. Deutschmann, J. Spielmann, S. Tischer, U. Kramm, H. Nirschl, O. Deutschmann, Iron as recyclable metal fuel: Oxidation of iron particles and the effect of cyclization, in preparation (2023).

[14] D. Spreitzer, J. Schenk, Reduction of Iron Oxides with Hydrogen—A Review, steel research int. 90 (10) (2019). doi:10.1002/srin.201900108.

[15] X. Liu, X. Zhang, J. Li, Q. Zhu, N. G. Deen, Y. Tang, Regeneration of iron fuel in fluidized beds Part II: Reduction experiments, Powder Technol. 420 (2023) 118183. doi:10.1016/j.powtec.2022.118183.

[16] C. Hessels, T. Homan, N. G. Deen, Y. Tang, Reduction kinetics of combusted iron powder using hydrogen, Powder Technol. 407 (2022) 117540. doi:10.1016/j.powtec.2022.117540.

[17] L. F. Calvo, G. Grasa, M. Alonso, M. E. Diego, Investigation on the performance of fine iron ore particles for energy storage applications in a novel CLC reactor, Fuel Process. Technol. 245 (2023) 107755. doi:10.1016/j.fuproc.2023.107755.

[18] C. Hessels, A. Smeets, G. Finotello, N. G. Deen, Y. Tang, Sintering behavior of combusted iron powder in a packed bed reactor with nitrogen and hydrogen, Particuology 83 (2023) 8–17. doi:10.1016/j.partic.2023.02.007.

[19] C. Hertel, P. Heidebrecht, K. Sundmacher, Experimental quantification and modelling of reaction zones in a cyclic watergas shift reactor, Int. J. Hydrogen Energy 37 (3) (2012) 2195–2203. doi:10.1016/j.ijhydene.2011.10.085.

[20] P. Heidebrecht, K. Sundmacher, Thermodynamic analysis of a cyclic water gas-shift reactor (CWGSR) for hydrogen production, Chem. Eng. Sci. 64 (23) (2009) 5057–5065. doi:10.1016/j.ces.2009.08.011.

Declaration of interests

☒ The authors declare that they have no known competing financial interests or personal relationships that could have appeared to influence the work reported in this paper.

☐ The authors declare the following financial interests/personal relationships which may be considered as potential competing interests: